

# Forward coherent $\omega$ and $\phi$ mesons production in the photon induced reaction on nuclei

Swapan Das <sup>1</sup>

*Nuclear Physics Division, Bhabha Atomic Research Centre,  
Trombay, Mumbai: 400085, India*

*Homi Bhabha National Institute, Anushakti Nagar, Mumbai-400094, India*

## Abstract

The differential cross sections of the forward coherent  $\omega$  and  $\phi$  mesons photoproduction from nuclei have been calculated using the Glauber model for the nuclear reaction. The measured cross section of the elementary reaction, i.e.,  $\gamma N \rightarrow \omega(\phi)N$  reaction, are used as input in the Glauber model. The experimentally determined free-space scattering parameters of the quoted mesons have been used to evaluate the meson nucleus interactions. The sensitivity of the cross section to the Fermi-motion of the nucleon and the nucleon-nucleon short-range correlation in the nucleus are studied. The calculated results are compared with the measured cross sections.

## 1 Introduction

The coherent meson production in the nuclear reaction provides opportunities to learn enriched physics associated the dynamics of the reaction. In the resonance region ( $\sim 1$ -2 GeV), the meson is originated due to the decay of the hadronic (or hyperonic) resonance produced in the nuclear reaction. Therefore, the properties of the resonance in a nucleus can be investigated by studying the coherent meson production in the nuclear reaction. The coherent pion produced in the  $\Delta(1232)$ -excitation region had been extensively used to study the  $\Delta$ -dynamics in the nucleus [1, 2, 3, 4]; as the branching ratio of this resonance decaying to the  $N\pi$  channel is 99.4% [5]. The  $\Delta$ -peak shift in the inclusive nuclear reaction (e.g.,  $({}^3\text{He}, t)$  reaction on the nucleus) relative to the  $pp$  collision [6] has been understood due to the coherent  $\pi^+$  meson production in the reaction [4]. The coherent pion cannot be produced in the  $pp$  reaction. Córdoba et al., [2] have emphasized that the  $\pi^0$  meson coherently produced in the  $(p, p')$  reaction on a nucleus can be used as beam. The coherent pion production (arising due to  $\Delta$ -decay) parallel to the momentum transfer to the nucleus is suppressed in the photo- and electro-induced nuclear reactions, unlike that occurred in the hadron induced nuclear reaction [2, 3]. The  $\Delta$ -renormalization in the nucleus leads to the reduction of the cross section of the coherent double pion  $\pi\pi$

---

<sup>1</sup>email: swapand@barc.gov.in

photoproduction from the nucleus, and that also modifies the shape of the pion energy distribution spectrum [7].

The coherent  $\eta$  meson production from the nucleus has been used to investigate the dynamics of the resonances heavier than  $\Delta(1232)$ . The  $N(1520)$  resonance (though possessing negligibly small branching ratio  $\sim 0.08\%$  in the  $N\eta$  channel [5]) contributes dominantly to the coherent  $\eta$  meson photoproduction from the spin-isospin saturated nucleus [8]. It should be mentioned that the resonance  $N(1535)$  has large branching ratio  $\sim 50\%$  in the  $N\eta$  channel [5], but that is suppressed in the quoted reaction because the  $\gamma NN(1535)$  coupling constants for the proton and neutron in the nucleus substantially cancel each other [9, 10]. The consideration of the non-local effect leads to the sizeable contribution of the  $N(1535)$  resonance in the stated reaction [9]. The importance of the  $t$ -channel  $\omega$  meson-exchange interaction in the above reaction is elucidated in Refs. [9, 10]. The contributions of the hadronic resonances to the coherently produced  $\eta$  meson in the proton nucleus collision have been explored [11], which reveal the dominant contribution to the coherent  $\eta$  meson production arises due to the decay of  $N(1520)$ , specifically, at high energy. In search of  $\eta$ -mesic nucleus, the importance of  $N(1535)$  resonance is mentioned in the coherent  $\eta$  meson photoproduction from  ${}^3\text{He}$  nucleus [12].

Beyond the resonance region, the coherent photoproductions of the  $\omega$  and  $\phi$  mesons from the deuteron at high momentum transfer region could not be explained by considering only the single scattering of the meson but those are realized by including the double scattering of the meson [13, 14]. The semi-hadronic decays of the  $\rho^0$  and  $\omega$  mesons coherently photoproduced in the nucleus demonstrates the enhancement in the cross section away from the peak region due to the interference of these mesons [15]. The coherent  $\rho$  meson photoproduction from the nucleus was studied to extract the informations about the  $\rho - N$  coupling constant,  $\rho - N$  scattering amplitude and  $N - N$  correlation in the nucleus [16]. The modification of the hadronic parameters (i.e., mass and width) is looked for the  $\rho$  and  $\omega$  mesons coherently produced in the photonuclear reactions [17].

The nuclear effect on the vector meson scattering parameters (i.e., the ratio of the real to imaginary part of the vector meson nucleon scattering amplitude  $\alpha_{VN}^*$  and the vector meson nucleon scattering cross section  $\sigma_t^{*VN}$  in the nucleus) is investigated by studying the nuclear mass number  $A$  dependent forward coherent four-momentum transfer cross section  $\frac{d\sigma_{coh}^{\gamma V}}{dq^2}(0)$  of the  $\gamma A \rightarrow VA$  reaction. The symbol  $V$  is used to represent a vector meson, e.g., either  $\omega$  or  $\phi$  meson. Using the vector meson dominance (VMD) model for the production of the quoted meson in the Glauber model, Sibirtsev et al., [18, 19] have analyzed the measured  $\frac{d\sigma_{coh}^{\gamma V}}{dq^2}(0)$  [20, 21] to extract  $\alpha_{VN}^*$  and  $\sigma_t^{*VN}$  for the  $\omega$  and  $\phi$  mesons. The Fermi-motion and short-range correlation of the nucleons in the nucleus are not considered in this analysis.

The quoted data for  $\frac{d\sigma_{coh}^{\gamma V}}{dq^2}(0)$  [20, 21] have been reanalyzed using Glauber model where

the production of the  $\omega$  and  $\phi$  mesons has been described by the respective measured forward four-momentum transfer cross section (i.e.,  $\frac{d\sigma}{dq^2} \gamma N \rightarrow \omega N$  and  $\frac{d\sigma}{dq^2} \gamma N \rightarrow \phi N$ ) of the photonucleon reaction. The experimentally determined free-space scattering parameters (i.e.,  $\alpha_{VN}$  and  $\sigma_t^{VN}$ ) for the above mesons are used to evaluate the distortion arising due to the meson nucleus interaction. The sensitivity of the calculated cross section  $\frac{d\sigma_{coh}^{\gamma V}}{dq^2}(0)$  to the Fermi-motion and short-range correlation of the nucleons in the nucleus has been investigated. The formalism of the reaction has been presented in sec. 2. The calculated results are discussed and compared with the data in sec. 3. The last section, i.e., sec. 4, ends with the conclusion.

## 2 Formalism

The differential cross section  $\frac{d\sigma_{coh}^{\gamma V}}{dq^2}$  of the four-momentum transfer distribution for the coherent vector meson production in the photonuclear reaction, according to Glauber model [22, 23], is given by

$$\frac{d\sigma_{coh}^{\gamma V}}{dq^2} = \frac{d\sigma}{dq^2} \gamma N \rightarrow V N \left| \int \dots \int d\mathbf{b} dz \varrho(b, z) e^{i(\mathbf{q}_\perp \cdot \mathbf{b} + q_\parallel z)} D_{k_V}^{(-)*}(b, z) \right|^2, \quad (1)$$

where  $V$  denotes either  $\omega$  or  $\phi$ , as mentioned earlier.  $q^2$  is the four-momentum transfer to the nucleus.  $q_\parallel$  and  $\mathbf{q}_\perp$  are the parallel and perpendicular components of the momentum transfer vector.  $\varrho(b, z)$  is the density distribution of the nucleus, normalized to the mass number of the nucleus.

$\frac{d\sigma}{dq^2} \gamma N \rightarrow V N$  in the above equation represents the cross section for the four-momentum transfer distribution in the elementary  $\gamma N \rightarrow V N$  reaction. The Glauber model is based on the fixed scatterer or frozen nucleon approximation [24]. Therefore, the Fermi-motion of the nucleon in the nucleus has been incorporated replacing  $\frac{d\sigma}{dq^2} \gamma N \rightarrow V N$  by that in the nucleus, i.e.,  $\left\langle \frac{d\sigma}{dq^2} \gamma N \rightarrow V N \right\rangle_A$ . For the beam energy  $E_\gamma$  and forward emission of the vector meson, it can be written as

$$\left\langle \frac{d\sigma}{dq^2} \gamma N \rightarrow V N \right\rangle_A (0, E_\gamma) = \int \int d\mathbf{k}_N d\epsilon_N S_A(\mathbf{k}_N, \epsilon_N) \frac{d\sigma}{dq^2} \gamma N \rightarrow V N (0, E'_\gamma), \quad (2)$$

with

$$\begin{aligned} E'_\gamma &= \frac{s - m_N^{*2}}{2m_N^*}; \quad m_N^* = m_N - \epsilon_N, \\ s &= (E_\gamma + E_N)^2 - (\mathbf{k}_\gamma + \mathbf{k}_N)^2, \\ E_N &= m_A - \sqrt{(k_N)^2 + (m_A - m_N^*)^2}. \end{aligned}$$

The spectral function  $S_A(\mathbf{k}_N, \epsilon_N)$  of the nucleus, normalized to unity, describes the probability of a nucleon with momentum  $\mathbf{k}_N$  and binding energy  $\epsilon_N$  in the nucleus [25].  $S_A(\mathbf{k}_N, \epsilon_N)$  for various nuclei are discussed elaborately in Ref. [26]. Therefore, those have not been presented explicitly.

$D_{k_V}^{(-)*}(b, z)$  in Eq. (1) describes the distortion arising due to the interaction of the vector meson with the nucleus. According to the eikonal description in the Glauber model [15, 24], it is given by

$$D_{k_V}^{(-)*}(b, z) = \exp \left[ -\frac{i}{v_V} \int_z^\infty dz' V_{OV}(b, z') \right], \quad (3)$$

where  $V_{OV}$  denotes the optical potential due to the meson nucleus interaction. It can be expressed as

$$\frac{1}{v_V} V_{OV}(b, z') = -\frac{1}{2}(\alpha_{VN} + i)\sigma_t^{VN} \varrho(b, z'), \quad (4)$$

with  $\alpha_{VN}$  representing the ratio of the real to imaginary part of the forward scattering amplitude  $f_{VN \rightarrow VN}(0)$  of the elementary  $VN \rightarrow VN$  reaction in the free-space.  $\sigma_t^{VN}$  denotes the total vector meson nucleon scattering cross section:  $\sigma_t^{VN} = \frac{4\pi}{k_V} f_{VN \rightarrow VN}(0)$ .

It should be mentioned that the nucleons bound in the nucleus do not occupy the same spatial region (called nuclear granularity [27]) because of the nucleon-nucleon short-range correlation which arises due to the repulsive (short-range) interaction between the nucleons in the nucleus. This correlation prevents the shadowing of the vector meson nucleon interaction due to the surrounding nucleons present in the nucleus. To include the nucleon-nucleon short-range correlation,  $\varrho(b, z')$  in Eq. (4) must be replaced [27] as

$$\varrho(b, z') \rightarrow \varrho(b, z')C(l), \quad (5)$$

where  $C(l)$  representing the correlation function depends on the path-length  $l(=|z' - z|)$  traversed by the vector meson. The nuclear matter estimation for  $C(l)$  [27, 28] is

$$C(l) = \left[ 1 - \frac{h(l)^2}{4} \right]^{1/2} [1 + f(l)], \quad (6)$$

with

$$h(l) = 3 \frac{j_1(k_F l)}{k_F l} \text{ and } f(l) = -e^{-\alpha l^2} (1 - \beta l^2). \quad (7)$$

The values of the parameters  $\alpha$  and  $\beta$  are 1.1 and  $0.68 \text{ fm}^{-2}$  respectively. The Fermi momentum is taken equal to  $1.36 \text{ fm}^{-1}$ . This simplified version of the correlation function agrees well with those derived using detail many-body calculations [27].

### 3 Result and Discussions

The differential cross sections  $\frac{d\sigma^{\gamma V}}{dq^2}(0)$  of the forward coherent vector mesons, i.e.,  $\omega$  and  $\phi$  mesons, photoproduction from nuclei have been calculated using Glauber model in the multi-GeV region. The cross sections are also evaluated considering the Fermi-motion of the nucleon and the nucleon-nucleon short-range correlation in the Glauber model. The energy dependent measured cross section for the forward vector meson production in the  $\gamma N \rightarrow VN$  reaction, i.e.,  $\frac{d\sigma^{\gamma N \rightarrow VN}}{dq^2}$  used in Eqs. (1) and (2), are taken from Refs. [19, 29, 30]. The density distribution  $\rho(r)$  of deuteron is generated using its wavefunction due to Paris potential [31].  $\rho(r)$  for  $^{12}\text{C}$  nucleus is described by the harmonic oscillator Gaussian form, where as that for other nuclei (heavier than  $^{12}\text{C}$ ) is illustrated by the two-parameter Fermi distribution function [32].

The optical potential  $V_{OV}$  in Eq. (4) is evaluated using the free-space vector meson nucleon scattering parameters  $\alpha_{VN}$  and  $\sigma_t^{VN}$ . For the  $\omega$  meson,  $\alpha_{\omega N}$  is taken from the calculation of the additive quark model and Regge theory due to Donnachie and Landshoff [18] (see the references there in). The experimentally determined values of  $\sigma_t^{\omega N}$  are given in Refs. [18, 33]. Using the vector meson dominance model,  $\frac{d\sigma^{\gamma N \rightarrow \phi N}}{dq^2}(0)$  can be written [19, 34] as

$$\frac{d\sigma^{\gamma N \rightarrow \phi N}}{dq^2}(0) = \frac{\alpha_{em}}{16\gamma_\phi^2} \left( \frac{\tilde{k}_\phi}{\tilde{k}_\gamma} \right)^2 [1 + \alpha_{\phi N}^2] (\sigma_t^{\phi N})^2, \quad (8)$$

where  $\tilde{k}_\gamma$  and  $\tilde{k}_\phi$  are the momenta in the  $\gamma N$  and  $\phi N$  center of mass systems respectively, evaluated at the energy in the  $\gamma N$  center of mass system.  $\alpha_{em}(= 1/137.036)$  is the fine structure constant.  $\gamma_\phi(= 6.72)$  is related to the photon coupling to  $\phi$  meson [35], which is extracted from the measured  $\phi \rightarrow e^+e^-$  decay width [5] using the expression  $\Gamma(m_\phi)_{\phi \rightarrow e^+e^-} = \frac{\pi}{3} (\frac{\alpha_{em}}{\gamma_\phi})^2 m_\phi$  [35]. The energy dependent values of  $\sigma_t^{\phi N}$  have been evaluated using the experimentally determined values of  $\frac{d\sigma^{\gamma p \rightarrow \phi p}}{dq^2}(0)$  [19, 30] and  $\alpha_{\phi N} = -0.3$  [23] in the above equation.

The mass number  $A$  dependent cross sections  $(1/A)d\sigma_{coh}^{\gamma\omega}/dq^2(0)$  of the forward coherent  $\omega$  meson production in the photonuclear reactions, calculated at 3.9 GeV, are shown in Fig. 1. The short-dashed curve (labeled as GM) represents the calculated results due to Glauber model. The large-dashed curve (labeled as GM+FM) illustrates that due to the Fermi-motion of the nucleon considered in the Glauber model. This figure shows the decrease in the calculated cross section due to the Fermi-motion. It occurs because the measured forward  $\frac{d\sigma^{\gamma N \rightarrow \omega N}}{dq^2}(0, E_\gamma)$ , as shown in Refs. [19, 29], is very sensitive to the energy, i.e., the cross section sharply falls with the increase in the energy around  $E_\gamma = 3.9$  GeV. As explained in Eq. (2), the forward  $\frac{d\sigma^{\gamma N \rightarrow \omega N}}{dq^2}(0, E'_\gamma)$  is to be evaluated at the beam energy  $E'_\gamma$  ( $\neq E_\gamma$ ) while the Fermi-motion of the nucleon is considered.

The dot-dashed curve (labeled as GM+SR) denotes the calculated cross section due to the nucleon-nucleon short-range correlation (without Fermi-motion) incorporated in the Glauber model. It shows the cross section is drastically increased, i.e., the absorption of the  $\omega$  meson is reduced due to the short-range correlation of the nucleons in the nucleus. The solid curve (labeled as GM+FS) arises because of the inclusion of both effects (i.e., Fermi-motion and short-range correlation) in the Glauber model. The dashed and solid curves in the figure elucidate that the cross section increases for the nuclei  $A > 25$ . In Fig. 2, the calculated cross sections (described by the dashed and solid curves) are compared with the data [20].

The variation of the calculated forward coherent  $\phi$  meson photoproduction cross sections, i.e.,  $(1/A)d\sigma_{coh}^{\gamma\phi}/dq^2(0)$ , with nuclei at 6.4 and 8.3 GeV are presented in Fig. 3. The short-dashed curve (labeled as GM) shows the result calculated using Glauber model. The contribution of the Fermi-motion of the nucleon to the cross section (not shown in the figure) is found insignificant for both energies. It occurs since the elementary cross section, i.e.,  $\frac{d\sigma}{dq^2}^{\gamma N \rightarrow \phi N}(0, E'_\gamma)$  in Eq. (2), is not sensitive to the beam energy in the above mentioned energy region [19, 30]. This is unlike to that occurs for the  $\omega$  meson photoproduction at 3.9 GeV, as discussed earlier. The dot-dashed curve (labeled as GM+SR) shows the cross section (similar to that depicted for the  $\omega$  meson) increases due to the short-range correlation of the nucleons in the nucleus.

The cross section  $(1/A)d\sigma_{coh}^{\gamma\phi}/dq^2(0)$  calculated using the Glauber model (dashed curve) and that calculated considering the Fermi-motion and short-range correlation of the nucleons in the Glauber model (solid curve) have been presented along with the data [21] in Fig. 4. As mentioned earlier, the contribution of the Fermi-motion to the cross section is negligibly small. Therefore, the cross sections measured at 6.4 and 8.3 GeV (as shown in the figure) is better understood (especially for heavy nuclei) because of the nucleon-nucleon short-range correlation incorporated in the Glauber model.

## 4 Conclusions

The forward coherent vector ( $V$ ) mesons, i.e.,  $\omega$  and  $\phi$  mesons, production cross sections  $\frac{d\sigma_{coh}^{\gamma V}}{dq^2}(0)$  in the photonuclear reactions have been calculated in the multi-GeV region using Glauber model, where the measured forward cross section  $\frac{d\sigma}{dq^2}^{\gamma N \rightarrow V N}$  of the  $\gamma N \rightarrow V N$  reaction and the experimentally determined free-space scattering parameters  $\alpha_{VN}$  and  $\sigma_t^{VN}$  are used. The sensitivity of the cross section to the Fermi-motion and nucleon-nucleon short-range correlation of the nucleons in the nucleus is investigated. The calculated results for the  $\omega$  meson photoproduction from nuclei at 3.9 GeV show that the cross section is sensitive to both of these effects. The cross section decreases due to the Fermi-motion

where as that increases because of the nucleon-nucleon short-range correlation. The cross sections of the  $\phi$  meson photoproduction from nuclei at 6.4 and 8.3 GeV are found insensitive to the Fermi-motion, but those are considerably enhanced due to the short-range correlation. The cross sections  $\frac{d\sigma_{coh}^{\gamma V}}{dq^2}(0)$  calculated using the measured  $\frac{d\sigma^{\gamma N \rightarrow VN}}{dq^2}$ ,  $\alpha_{VN}$  and  $\sigma_t^{VN}$  for both  $\omega$  and  $\phi$  mesons are well accord with the data.

## 5 Acknowledgement

The author duly acknowledges Dr. S. M. Yusuf for his support to carry out this work.

## References

- [1] T. Ericson and W. Weise, Pions and Nuclei (Clarendon Press, Oxford, 1988), p. 242; E. Oset, H. Toki and W. Weise, Phys. Rept. **83** (1982) 281.
- [2] S. Das, Phys. Rev. C **66** (2002) 014604; P. F. de Córdoba, J. Nieves, E. Oset and M. J. Vicente-Vacas, Phys. Lett. B **319** (1993) 416; E. Oset, P. F. de Córdoba, J. Nieves, and M. J. Vicente-Vacas, Phys. Scr. **48** (1993) 101; V. F. Dmitriev, Phys. Rev. C **48** (1993) 357;
- [3] B. Körfggen, F. Osterfeld and T. Udagawa, Phys. Rev. C **50** (1994) 1637; S. Hirenzaki, J. Nieves, E. Oset and M. J. Vicente-Vacas, Phys. Lett. B **304** (1993) 198; S. S. Kamalov and T. D. Kaipov, Phys. Lett. B **162** (1985) 260; D. Drechsel, L. Tiator, S. S. Kamalov and S. N. Yang, Nucl. Phys. A **660** (1999) 423; B. Krusche et al., Phys. Lett. B **526** (2002) 287.
- [4] J. Chiba, et al., Phys. Rev. Lett. **67** (1991) 1982; T. Hennino, et al., Phys. Lett. B **303** (1993) 236.
- [5] M. Tanabashi, et al., (Particle Data Group), Phys. Rev. D **98** (2018) 030001; <http://pdg.lbl.gov./xsect/contents.html>.
- [6] D. Contardo, et al., Phys. Lett. B **168** (1986) 331; C. Gaarde, Annu. Rev. Nucl. Part. Sci. **41** (1991) 187.
- [7] S. S. Kamalov and E. Oset, Nucl. Phys. A **625** (1997) 873.
- [8] C. Bennhold and H. Tanabe, Nucl. Phys. A **530** (1991) 625.
- [9] W. Peters, H. Lenske and U. Mosel, Nucl. Phys. A **642** (1998) 506.
- [10] A. Fix and H. Arenhövel, Nucl. Phys. A **620** (1997) 457.
- [11] S. Das, Phys. Lett. B **737** (2014) 75; Phys. Rev. C **92** (2015) 014621.
- [12] F. Pheron et al., Phys. Lett. B **709** (2012) 21.
- [13] T. Chetry et al., Phys. Lett. B **782** (2018) 646; T. Mibe et al., Phys. Rev. C **76** (2007) 052202(R).
- [14] L. Frankfurt et al., Nucl. Phys. A **622** (1997) 511.
- [15] S. Das, Phys. Rev. C **94** (2016) 025204.

- [16] K. Gotteried and D. I. Julius, Phys. Rev. D **1** (1970) 140.
- [17] S. Das, Eur. Phys. J. A **49** (2013) 123; Phys. Rev. C **83** (2011) 064608.
- [18] A. Sibirtsev, Ch. Elster and J. Speth, arXiv:0203044 [nucl-th].
- [19] A. Sibirtsev, H.-W. Hammer, U.-G. Meißner and A. W. Thomas, Eur. Phys. J. A **29** (2006) 209.
- [20] T. J. Brodbeck et al., Nucl. Phys. B **136** (1978) 95.
- [21] G. McClellan et al., Phys. Rev. Lett. **26** (1971) 1593.
- [22] L. Frankfurt, M. Strikman and M. Zhalov, Phys. Rev. C **67** (2003) 034901.
- [23] T. H. Bauer, R. D. Spital, D. R. Yennie and F. M. Pipkin, Rev. Mod. Phys. **50** (1978) 261; Erratum, *ibid*, **51** (1979) 407.
- [24] R. J. Glauber, in Lectures in Theoretical Physics, Vol. 1, edited by W. E. Brittin et al., (Interscience, New York, 1959), p. 315; J. M. Eisenberg and D. S. Kolton, Theory of Meson Interaction with Nuclei (John Wiley & Sons, New York, 1980), p. 158.
- [25] E. Ya. Paryev, J. Phys. G **40** (2013) 025201.
- [26] E. Ya. Paryev, Eur. Phys. J. A **7** (2000) 127.
- [27] T.-S. H. Lee and G. A. Miller, Phys. Rev. C **45** (1992) 1863.
- [28] G. A. Miller and J. E. Spencer, Ann. Phys. (N.Y.) **100** (1976) 562.
- [29] A. Sibirtsev, K. Tsushima and S. Krewald, Phys. Rev. C **67** (2003) 055201; J. Barth et al., Eur. Phys. J. A **18** (2003) 117.
- [30] T. Mibe, et al., Phys. Rev. Lett. **95** (2005) 182001; J. Barth et al., Eur. Phys. J. A **17** (2003) 269.
- [31] M. Lacombe et al., Phys. Lett. B **101** (1981) 139.
- [32] C. W. De Jager, H. De Vries and C. De Vries, At. Data Nucl. Data Tables, **14** (1974) 479.
- [33] G. I. Lykasov, W. Cassing, A. Sibirtsev and M. V. Rzjanin, Eur. Phys. J. A **6** (1999) 71.

- [34] S. Das, Phys. Rev. C **96** (2017) 034616.
- [35] J. J. Sakurai, Currents and Mesons (The University of Chicago press, Chicago, 1969), p 48; R. K. Bhaduri, Models of the Nucleon (Addison-Wesley Publishing Company, Inc., California, 1988), p 261.

## Figure Captions

1. (color online). The calculated nuclear mass number  $A$  dependent cross sections of the forward coherent  $\omega$  meson production in the  $\gamma A$  reaction. Various curves in the figure are elaborated in the text.
2. (color online). The calculated results for the  $\omega$  meson are compared with the data [20]. The dashed curve describes the cross section calculated using Glauber model, where as the solid curve arises because of the Fermi-motion and short-range correlation of the nucleons in the nucleus incorporated in the Glauber model.
3. (color online). Same as those presented in Fig. 1 but for the  $\phi$  meson at different energies. Since the contribution of the Fermi-motion of the nucleon to the cross section is negligibly small, it is not shown in the figure.
4. (color online). Same as those in Fig. 2 but for the  $\phi$  meson at different energies. The data are taken from Ref. [21].

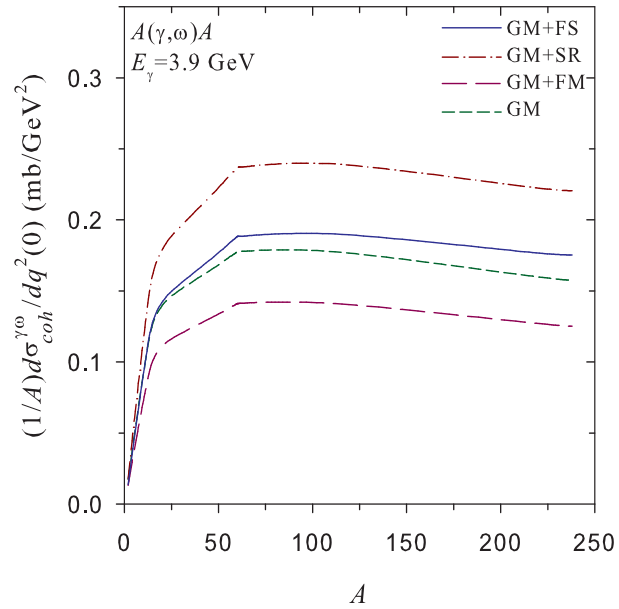


Figure 1: (color online). The calculated nuclear mass number  $A$  dependent cross sections of the forward coherent  $\omega$  meson production in the  $\gamma A$  reaction. Various curves in the figure are elaborated in the text.

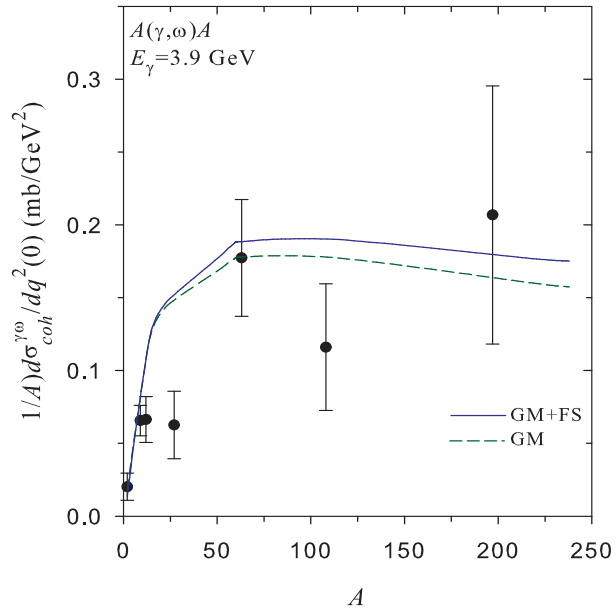


Figure 2: (color online). The calculated results for the  $\omega$  meson are compared with the data [20]. The dashed curve describes the cross section calculated using Glauber model, where as the solid curve arises because of the Fermi-motion and short-range correlation of the nucleons in the nucleus incorporated in the Glauber model.

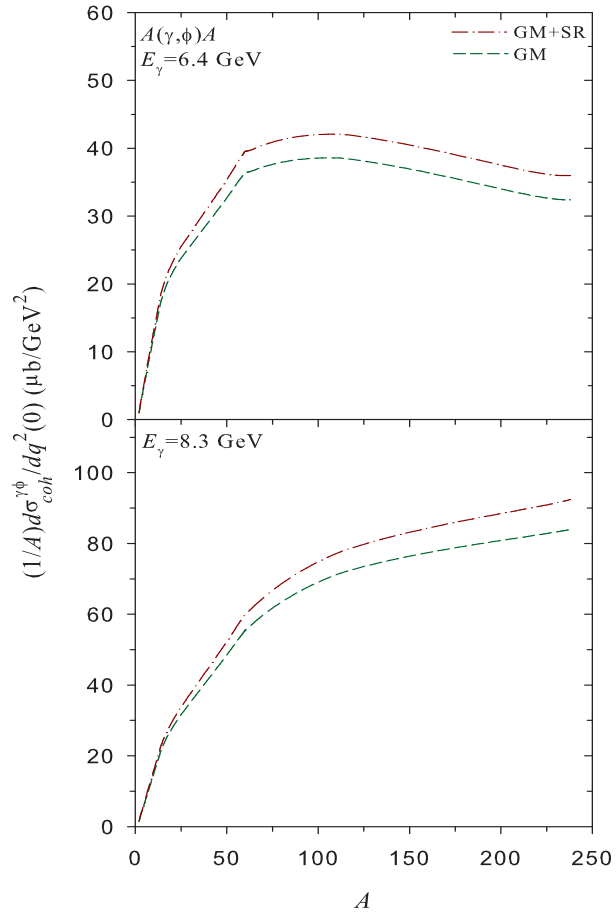


Figure 3: (color online). Same as those presented in Fig. 1 but for the  $\phi$  meson at different energies. Since the contribution of the Fermi-motion of the nucleon to the cross section is negligibly small, it is not shown in the figure.

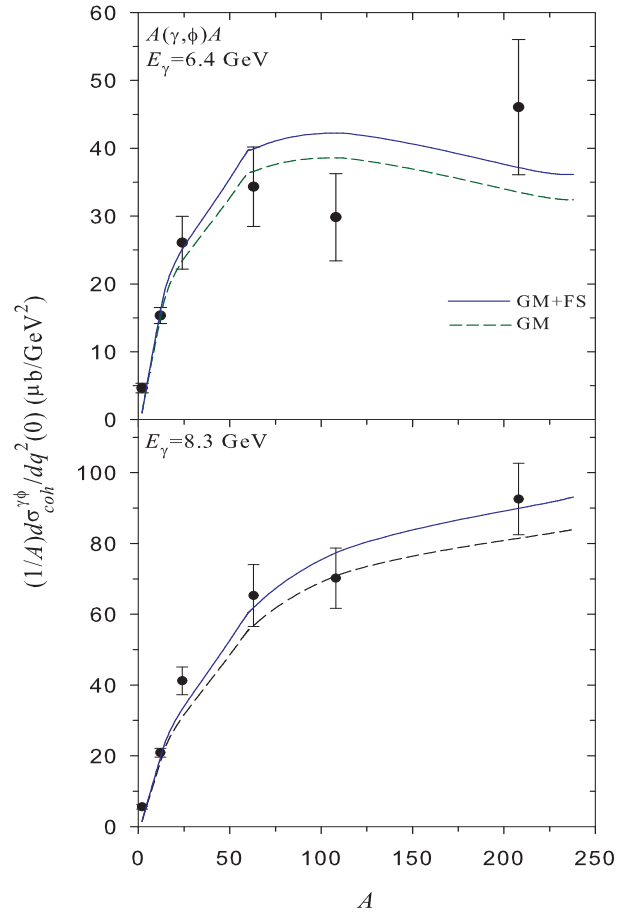


Figure 4: (color online). Same as those in Fig. 2 but for the  $\phi$  meson at different energies. The data are taken from Ref. [21].